THE JOURNAL OF BIOLOGICAL CHEMISTRY VOL. 287, NO. 20, pp. 16530–16540, May 11, 2012
© 2012 by The American Society for Biochemistry and Molecular Biology, Inc. Published in the U.S.A.

Calmodulin Bound to the First IQ Motif Is Responsible for Calcium-dependent Regulation of Myosin 5a*[S]

Received for publication, January 15, 2012, and in revised form, March 5, 2012 Published, JBC Papers in Press, March 21, 2012, DOI 10.1074/jbc.M112.343079

Zekuan Lu[1], **Mei Shen**[1], **Yang Cao, Hai-Man Zhang, Lin-Lin Yao, and Xiang-dong Li**[2]

From the Group of Cell Motility and Muscle Contraction, National Laboratory of Integrated Management of Insect Pests and Rodents, Institute of Zoology, Chinese Academy of Sciences, Beijing 100101, China

Background: Myosin 5a ATPase activity is regulated by calcium.
Results: The ATPase of the truncated myosin 5a having the motor domain and the first IQ motif is inhibited by its tail in a calcium-dependent manner.
Conclusion: The calmodulin in the first IQ motif of myosin 5a is responsible for calcium-dependent regulation.
Significance: This presents a new paradigm for calcium regulation of unconventional myosins.

Myosin 5a is as yet the best-characterized unconventional myosin motor involved in transport of organelles along actin filaments. It is well-established that myosin 5a is regulated by its tail in a Ca^{2+}-dependent manner. The fact that the actin-activated ATPase activity of myosin 5a is stimulated by micromolar concentrations of Ca^{2+} and that calmodulin (CaM) binds to IQ motifs of the myosin 5a heavy chain indicates that Ca^{2+} regulates myosin 5a function via bound CaM. However, it is not known which IQ motif and bound CaM are responsible for the Ca^{2+}-dependent regulation and how the head-tail interaction is affected by Ca^{2+}. Here, we found that the CaM in the first IQ motif (IQ1) is responsible for Ca^{2+} regulation of myosin 5a. In addition, we demonstrate that the C-lobe fragment of CaM in IQ1 is necessary for mediating Ca^{2+} regulation of myosin 5a, suggesting that the C-lobe fragment of CaM in IQ1 participates in the interaction between the head and the tail. We propose that Ca^{2+} induces a conformational change of the C-lobe of CaM in IQ1 and prevents interaction between the head and the tail, thus activating motor function.

Myosin is a type of molecular motor protein that converts energy from ATP hydrolysis into mechanical movement along actin filaments. Myosin motor function must be tightly regulated in cells to transport cargo efficiently and to avoid futile hydrolysis of ATP. The regulation of muscle myosin (conventional myosin) is well established. Among more than 30 types of unconventional myosins, the regulation of vertebrate myosin 5a is best characterized.

Myosin 5a consists of two identical heavy chains that dimerize through coiled-coil structures to form a homodimer. The N-terminal ~760 amino acid residues form the motor domain containing ATP- and actin-binding sites. The motor domain is followed by a neck that consists of six IQ motifs with the consensus sequence IQ*XXX*R*G**XXX*R, which act as the binding sites for calmodulin (CaM)[3] or CaM-like light chains. The C-terminal ~900 amino acid residues form the tail. The proximal portion of the tail contains a series of coiled-coils separated by several flexible regions responsible for the dimerization of myosin 5a. The distal portion of the tail forms a globular tail domain (GTD). The tail mediates myosin 5a binding to specific membrane-bound organelles such as melanosomes (1–4).

A tail-inhibition model for the regulation of myosin 5a is generally accepted: myosin 5a in the inhibited state is in a folded conformation such that the tail domain interacts with and inhibits myosin 5a motor activity; high Ca^{2+} or cargo binding may reduce interaction between the head and tail domains, thus activating motor activity. This model is based on the following key findings. 1) The actin-activated ATPase activity of myosin 5a is stimulated by micromolar Ca^{2+}, whereas myosin 5a heavy meromyosin (HMM), lacking GTD, is constitutively active (5–7). 2) Analytical ultracentrifugation analysis showed that myosin 5a is in a 14 S-folded conformation under lower Ca^{2+} conditions and in an 11 S open conformation in the presence of micromolar Ca^{2+} (6–8). In contrast, there is no such transition for the truncated myosin 5a lacking GTD (6–8). 3) Negative staining electron microscopy showed that myosin 5a molecules form a triangular conformation in which the motor domain contacts the GTD, and that myosin 5a HMM molecules form an extended conformation (7, 9–10). 4) The isolated GTD is capable of inhibiting the ATPase activity of myosin 5a HMM, and the inhibition is abolished by high Ca^{2+} (9–11). 5) Melanophilin, the cargo-binding protein for myosin 5a in melanosome, binds to the tail of myosin 5a and is capable of stimulating the ATPase activity of myosin 5a (4).

The fact that the actin-activated ATPase activity of myosin 5a is stimulated by micromolar concentrations of Ca^{2+} and CaM binds to IQ motifs of myosin 5a heavy chain indicate that Ca^{2+} regulates myosin 5a function via the bound CaM (5–6).

* This work was supported by National Natural Science Foundation of China (No. 31171367 and 31071973), Hundred Talent Program from Chinese Academy of Sciences, and National Basic Research Program of China (No. 2012CB114102).
[S] This article contains supplemental Figs. S1–S6.
[1] Both authors contributed equally to this work.
[2] To whom correspondence should be addressed: Institute of Zoology, Chinese Academy of Sciences, Beijing, 100101, China. Tel.: 86-10-6480-6015; E-mail: lixd@ioz.ac.cn or lixd001@gmail.com.

[3] The abbreviations used are: CaM, calmodulin; GTD, globular tail domain of myosin 5a; GST-GTD, GST fusion protein of GTD; HMM, heavy meromyosin; MD, motor domain; RLC, regulatory light chain; S1, subfragment 1 of myosin.

However, it is not known which IQ motif and bound CaM is responsible for the regulation, nor how the head-tail interaction is affected by Ca^{2+}. It appears that activation of ATPase activity of myosin 5a by high Ca^{2+} is correlated with Ca^{2+}-induced dissociation of CaM from a single specific IQ motif (12). Several groups identified the specific IQ motif to be the second IQ motif (IQ2) and proposed that Ca^{2+}-dependent regulation of myosin 5a is via the CaM in IQ2 (13–16). This hypothesis seems plausible since the regulation of scallop myosin and smooth muscle myosin is initiated from the regulatory light chain (a CaM-like light chain) bound to IQ2 (17–19). However, there is no direct evidence to support this hypothesis.

Recently, we proposed a model for the interaction between the head and the GTD of myosin 5a based on mutagenesis analysis of the highly conserved charged residues in the motor domain and the GTD on the regulation (11). In our model, we assign the GTD-binding site to a pocket of the motor domain, formed by the N-terminal domain, converter, and the CaM in the first IQ motif (IQ1). This assignment immediately suggests a possible mechanism for Ca^{2+}-dependent regulation of myosin 5a: the CaM in IQ1 is part of or close to the GTD-binding pocket and Ca^{2+}-induced conformational change of CaM in IQ1 may prevent the interaction between the motor domain and the GTD, thus activating motor function. Of course, this model could not exclude the possibility that Ca^{2+}-induced activation is initiated from the CaM in IQ2 and transferred to the CaM in IQ1 through the interaction between these two CaMs. In the present study, we provide direct evidence that it is the CaM in IQ1, but not the one in IQ2, responsible for the regulation of myosin 5a by Ca^{2+}.

EXPERIMENTAL PROCEDURES

Materials—Restriction enzymes and modifying enzymes were purchased from New England BioLabs (Beverly, MA), unless indicated otherwise. Actin was prepared from rabbit skeletal muscle acetone powder according to Spudich and Watt (20). Ni-NTA-agarose was purchased from Qiagen (Hilden, Germany). Anti-FLAG M2 antibody, Anti-FLAG M2 affinity gel, phosphoenol pyruvate, 2,4-dinitrophenyl-hydrazine, and pyruvate kinase were from Sigma. FLAG peptide (AspTyrLysAspAspAspAspLys) was synthesized by Augct Co. (Beijing, China). Phenyl-Sepharose 6 Fast Flow and Glutathione-Sepharose 4 Fast Flow were from GE Healthcare. Oligonucleotides were synthesized by Invitrogen. GST-GTD was prepared as described previously (10).

Myosin 5a Expression Vectors—All myosin 5a constructs in this study were created from a melanocyte isoform of myosin 5a cDNA(21). M5aΔT and M5aHMM with N-terminal His-tag and Flag-tag were prepared as described previously (10). C-terminal-truncated myosin 5a constructs were produced by introducing a stop codon at various nucleotide sites (Fig. 1). M5aΔT-IQ26 was created by substituting IQ2 (aa 788–812) in M5aΔT with IQ6 (aa 884–908). MD-IQ1/6 was created by substituting IQ2 (aa 788–815) in MD-IQ1/2 with IQ6 (aa 884–908). MD-IQ3 and MD-IQ5 were created by substituting IQ1 (aa 765–787) in MD-IQ1 with IQ3 (aa 813–835) and IQ5 (aa 861–883), respectively. Recombinant baculoviruses were prepared using Bac-To-Bac system (Invitrogen) as described previously (6, 10).

Expression and Purification of Myosin 5a Constructs—Sf9 cells were coinfected with the recombinant viruses of myosin 5a heavy chain and CaM wild type or mutants. The expressed myosin 5a was purified by anti-Flag M2 affinity chromatography as described previously (6, 10). The concentrations of the purified myosin 5a were determined by absorbance at 280 nm, using the following molar extinction coefficients (liters·mol^{-1}·cm^{-1}): 167510 (M5aΔT), 164950 (M5aΔT-IQ26), 150300 (M5aHMM), 141220 (MD-IQ1–6), 106560 (MD-IQ1/2), 104000 (MD-IQ1/6), 100040 (MD-IQ1), 96080 (MD-IQ1-short), 90270 (MD), 102360 (MD-IQ3), and 101080 (MD-IQ5). These molar extinction coefficients were calculated based on the amino acid composition of myosin 5a heavy chain and the bound CaM. In the case where the absorbance at 280 nm was lower than 0.5 or the absorbance spectrum was aberrant, the protein concentration was determined by SDS-PAGE and Coomassie Brilliant Blue staining with known concentrations of myosin 5a protein as a standard.

Expression and Purification of CaM Wild Type and Variants—The cDNA for human CaM was obtained by PCR and subcloned into pFastBac or pT7 vector. CaM mutations abolishing Ca^{2+}-binding sites, including B12Q (mutation of E31Q/E67Q), B34Q (mutations of E104Q/E140Q), and B1234Q (mutations of E31Q/E67Q/E104Q/E140Q) were introduced by QuikChange site-directed mutagenesis with Ultra High Fidelity Pfu (Stratagene, CA) and standard molecular biological techniques. The CaM in pFastBac was used for preparing recombinant baculovirus by using Bac-To-Bac system (Invitrogen). The CaM in pT7 was used for expressing CaM in *Escherichia coli*.

CaM wild type and B12Q mutant were expressed in BL21(DE3) and purified according to a published method using affinity chromatography on phenyl-Sepharose (22). Phenyl-Sepharose chromatography could not be used for CaM-B34Q and -B1234Q mutants, and therefore an alternative purification scheme, based on that of smooth muscle myosin regulatory light chain (23), was devised as described below.

BL21(DE3) was transformed with CaM in pT7 expression vector and then cultured in 200 ml of LB medium supplemented with 50 μg/ml ampicillin at 37 °C until the $A_{600\ nm}$ was 0.8–1.0. About 0.2 mM isopropyl-1-thio-β-D-galactopyranoside (IPTG) was added to the liquid culture, and the cells were cultured overnight. After two freeze-thaw treatments, the harvested cells were suspended in 20 ml of lysis buffer (50 mM Tris-HCl, pH 7.5, 2 mM EDTA, 1 mM DTT, and 1 mg/ml lysozyme) and incubated for 1 h (all experiments were done at 4 °C unless otherwise indicated). To decrease the viscosity of cell lysates, 3 mM $MgCl_2$ and 20 units/ml DNase I were added to digest DNA. Cell lysates were clarified by centrifugation (15,000 rpm for 15 min). Unwanted protein in the supernatant was precipitated by adding 3% TCA and adjusting to pH 5.3 with 10 N NaOH, and removed by centrifugation (10,000 rpm for 10 min). CaM in the supernatant was precipitated by increasing TCA to 6% and collected by centrifugation (10,000 rpm for 10 min). The pellet was dissolved in 10 ml of 30 mM Tris-HCl, pH 7.5 (adjusting pH with 1 M Tris-base). After dia-

lyzing against 1 liter of Buffer A (50 mM Tris-HCl, pH 7.5 and 1 mM DTT) overnight and centrifugation at 10,000 rpm for 10 min, the supernatant was loaded onto a DEAE-Sepharose column (1.5 cm × 11 cm). After washing with buffer A, the bound proteins were eluted with 120 ml of Buffer-A containing a linear NaCl gradient from 0 to 500 mM. The fractions containing CaM were determined by SDS-PAGE analysis, concentrated, dialyzed against Buffer D (30 mM Tris-HCl, pH 7.5, 30 mM NaCl, and 1 mM DTT), and stored at −80 °C. CaM concentrations were determined by the absorbance at 280 nm ($1A_{280}$ is equal to 5.26 mg/ml CaM).

CaM-C (the C-lobe of CaM, aa 80–148) was prepared similarly to wild type CaM, except that 2 M NaCl instead of 0.3 M NaCl was used for binding of CaM-C with phenyl-Sepharose. CaM-C concentration was determined by the absorbance at 280 nm ($1A_{280}$ is equal to 3.28 mg/ml CaM-C). CaM-N (the N-lobe of CaM, aa 1–79) was prepared by precipitation with TCA without chromatography. Briefly, BL21(DE3) was transformed with CaM-N in pT7 expression vector and then cultured in 1 liter of LB medium supplemented with 50 μg/ml ampicillin and induced by IPTG. After two freeze-thaw treatments, the harvested cells were suspended in 80 ml of lysis buffer (50 mM Tris-HCl, pH 7.5, 2 mM EDTA, 1 mM DTT, and 1 mg/ml lysozyme) and incubated for 1 h and digested with DNase as above. Cell lysates were clarified by centrifugation (15,000 rpm for 15 min). Unwanted protein in the supernatant was precipitated by adding 3% TCA and adjusting to pH 5.3 with 10 N NaOH, and removed by centrifugation (10,000 rpm for 10 min). The TCA concentration in the supernatant was increased to 6% to precipitate the remaining unwanted proteins, which were removed by centrifugation. CaM-N in the supernatant was then precipitated by increasing TCA to 10% and collected by centrifugation. The pellet was dissolved in ~1 ml of 1 M Tris-HCl, pH 7.5 and clarified by centrifugation. The supernatant was loaded onto a Sephadex G25 column pre-equilibrated with Buffer-D for buffer exchange. Since CaM-N does not contain aromatic amino acid residues, its protein concentration was estimated by SDS-PAGE (4–20%) with purified CaM-C as standard.

ATPase Assay—The ATPase activity of myosin 5a was measured in a plate-based, ATP regeneration system as described previously with slight modification (11). Unless otherwise indicated, the ATPase activities of myosin 5a were measured in a solution containing 20 mM MOPS-KOH, pH 7.0, 50 mM NaCl, 1 mM $MgCl_2$, 1 mM DTT, 0.25 mg/ml BSA, 12 μM CaM, 0.5 mM ATP, 2.5 mM PEP, 20 units/ml pyruvate kinase, 20–50 nM truncated myosin 5a, 40 μM actin, various concentrations of GST-GTD, and 1 mM EGTA at 25 °C. For pCa4 conditions, 1 mM EGTA was replaced by 0.87 mM EGTA and 1 mM $CaCl_2$. To measure the ATPase activity of MD-IQ1 with CaM variant, the corresponding CaM variant was included in the assay in place of wild type CaM. The inhibition of ATPase activities by GST-GTD was fitted with a quadratic equation or hyperbolic equation to obtain the K_d between the myosin 5a head and GST-GTD as described previously (11).

Actin Cosedimentation Assay—Purified myosin 5a constructs were incubated with rabbit skeletal actin (10 μM) in a 50 μl solution consisting of 20 mM MOPS-KOH, pH7.0, 50 mM NaCl, 1 mM $MgCl_2$, 1 mM DTT, 12 μM CaM WT, or mutants, and 1 mM EGTA (1 mM EGTA was replaced with 0.87 mM EGTA and 1 mM $CaCl_2$ for pCa4 conditions) at 0 °C for 10 min and then centrifuged in a benchtop ultracentrifuge (Beckman Optima MAX-XP) at 80,000 rpm for 10 min at 0 °C. The pellets were resuspended in 50 μl of SDS-gel sample buffer (containing 5 mM EGTA) and subjected to SDS-PAGE. The amounts of the myosin 5 heavy chain and CaM were determined by NIH Image J 1.42Q (Bethesda, MD).

Electrophoretic Mobility Shift of CaM—CaM and its variants display unique electrophoretic mobility shift in SDS-PAGE in response to Ca^{2+} (24). Before applied to SDS-PAGE (15%), the purified CaM variants and the purified MD-IQ1 coexpressed with CaM variants were incubated with 5 mM EGTA or 5 mM $CaCl_2$ on ice for 30 min, then mixed with SDS loading buffer and boiled for 5 min. Protein bands were visualized by Coomassie Brilliant Blue staining.

RESULTS

The IQ1 Motif but Not IQ2 Motif Is Critical for the Regulation of Myosin 5a by Ca^{2+}—To investigate the regulation of myosin 5a, we produced a number of truncated myosin 5a (Fig. 1). We coexpressed the truncated myosin-5 with CaM and purified them with Anti-FLAG affinity chromatography. The apparent molecular masses of the truncated myosins in SDS-PAGE agree well with the calculated values based on their sequences. All truncated myosins, except MD, were copurified with CaM (supplemental Fig. S1).

It is known that the association of CaM with IQ2 of myosin 5a is regulated by Ca^{2+}, and it was proposed that the Ca^{2+}-dependent regulation of myosin 5a is via the CaM in IQ2 (13–16). To test this possibility, we created M5aΔT-IQ26, a truncated myosin 5a having the globular tail domain (GTD) deleted and the IQ2 substituted with IQ6 (Fig. 1 and supplemental Fig. S1). We found that the actin-activated ATPase activity of M5aΔT-IQ26 is still inhibited by the GST-GTD in a Ca^{2+}-dependent manner, similar to that of M5aΔT with its authentic IQ motifs (supplemental Fig. S2). Thus, the substitution of IQ2 with IQ6 does not alter the regulation of myosin 5a. It is possible that, similar to that of IQ2, the association of CaM with IQ6 is also regulated by Ca^{2+}; thus the substitution of IQ2 with IQ6 does not alter the regulation. To test this possibility, we created MD-IQ1/6 by substituting IQ2 in MD-IQ1/2 with IQ6 (Fig. 1), and measured the association of CaM with MD-IQ1/2 and MD-IQ1/6. We found that high Ca^{2+} dissociates 43% CaM from MD-IQ1/2 and less than 5% CaM from MD-IQ1/6 (supplemental Fig. S3). These results are consistent with previous report, that IQ6 has high affinity to CaM in either low or high Ca^{2+} conditions (25). Therefore, Ca^{2+}-dependent dissociation of CaM from IQ2 is not responsible for the regulation of myosin-5a.

We previously found that the strong inhibition by the GTD requires the double-headed structure and an intact first coiled-coil segment (10). However, as pointed out by Thirumurugan *et al.* (9), we have noticed a reproducible, though weak, inhibition of myosin 5a S1 ATPase activity by the GTD (10), and this weak inhibition was abolished by high Ca^{2+}. Thus, there likely is a Ca^{2+}-dependent interaction between the GTD and myosin 5a S1. We expect that the weak inhibition of myosin 5a S1 by the

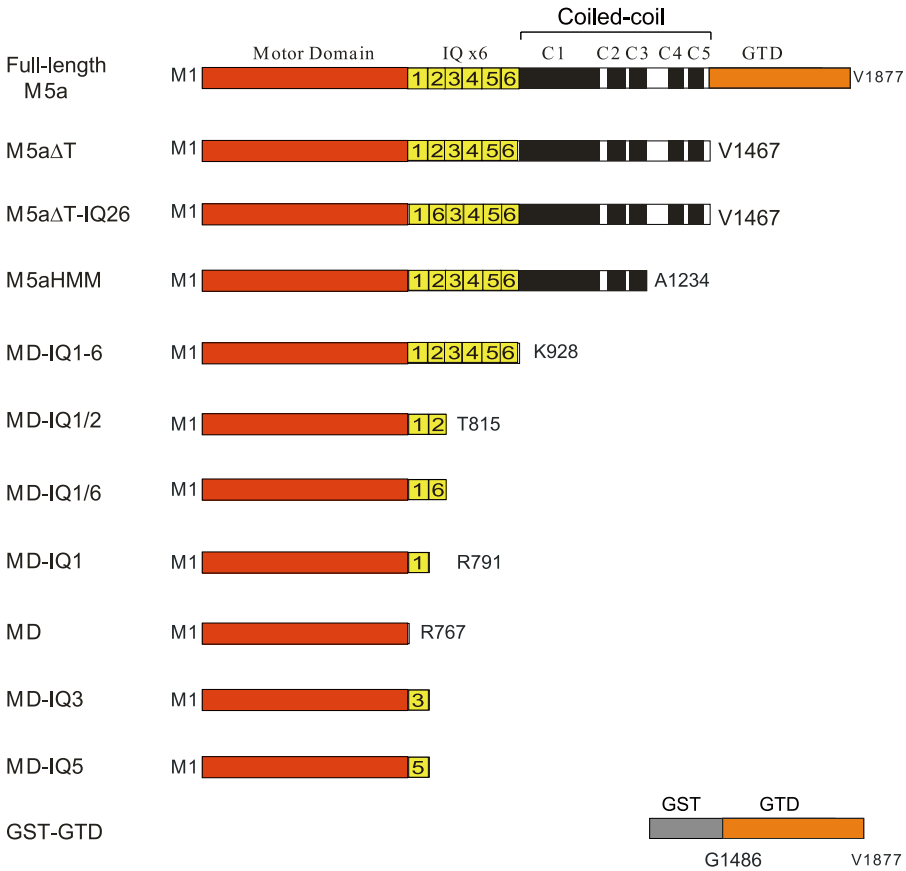

FIGURE 1. **Diagram of myosin 5a constructs studied in this report.** Amino acid numbers of the constructs are indicated. M5aΔT-IQ26 was created by substituting IQ2, in M5aΔT with IQ6. MD-IQ1/6 was created by substituting IQ2 in MD-IQ1/2 with IQ6. MD-IQ3 and MD-IQ5 were created by substituting IQ1 in MD-IQ1 with IQ3 and IQ5 respectively. For clarity, the diagram was not drawn to scale.

GTD could be used for dissecting the regulatory machinery of myosin 5a, and therefore we tried to enhance the inhibition of myosin 5a S1 by the GTD by altering the assay conditions.

We previously showed that inhibition of myosin 5a motor function by the GTD depends largely on ionic strength (6), *i.e.* high ionic strength attenuates the inhibition by the GTD. To quantify the effects of ionic strength on the inhibition by GST-GTD, we measured the inhibition of M5aHMM ATPase activity by GST-GTD in a range of 50 mM to 250 mM NaCl (supplemental Fig. S4). The calculated K_d for GST-GTD decreased from 11.3 μM at 250 mM NaCl to 14.8 nM at 50 mM NaCl. It is noteworthy that GST-GTD shows much higher affinity for M5aHMM than the monomeric GTD we used previously (10).

We expected that lower ionic strength might also enhance the weak inhibition of myosin 5a S1 by GST-GTD. Indeed, in EGTA conditions, 8 μM GST-GTD inhibits about 15% ATPase activity of myosin 5a S1 in 100 mM NaCl conditions and about 50% in 50 mM NaCl conditions. We therefore conducted all following ATPase assay in the presence of 50 mM NaCl.

The ATPase activity of MD-IQ1–6, a truncated myosin 5a with motor domain and intact IQ motifs, was significantly inhibited by GST-GTD in EGTA conditions, but not in pCa4 conditions (Fig. 2*A*). These results indicate that MD-IQ1–6 contains all components for Ca^{2+}-dependent regulation. On the other hand, the double-headed structure, although enhancing the interaction between the two heads and the two GTDs, is not essential for regulation.

To identify the IQ motif responsible for the regulation of myosin 5a by Ca^{2+}, we created a number of truncated myosin 5a S1 lacking various IQ motifs (Fig. 1 and supplemental Fig. S1), and examined the effects of GST-GTD and Ca^{2+} on the ATPase activities of these constructs. Similar to that of MD-IQ1–6, the ATPase activities of MD-IQ1/2 and MD-IQ1 are inhibited by GST-GTD in EGTA conditions, but not in pCa4 conditions (Fig. 2, *B* and *C*). By contrast, the ATPase activity of MD is not inhibited by GST-GTD in either EGTA or pCa4 conditions (Fig. 2*D*). Three truncated myosin 5a constructs, *i.e.* MD-IQ1-6, MD-IQ1-2, and MD-IQ1, are all inhibited by GST-GTD with a similar K_d, suggesting that CaM in IQ2-IQ6 does not directly participate in inhibitory formation and are dispensable for Ca^{2+}-dependent regulation. These results indicate that the CaM in IQ1 is responsible for the regulation of myosin 5a by Ca^{2+}.

In the absence of Ca^{2+}, GST-GTD inhibits the ATPase activities of MD-IQ1 but not that of MD, suggesting that the CaM bound to IQ1 participates in the interaction with GTD. This raises a possibility that the reversal of GST-GTD inhibition on MD-IQ1 by Ca^{2+} is due to Ca^{2+}-induced dissociation of CaM from IQ1. Alternatively, Ca^{2+} might induce a conformation change of CaM in IQ1 that reverses the inhibition by GST-GTD. To distinguish between these two possibilities, we compared the association of CaM with MD-IQ1 in the absence and presence of Ca^{2+}. About 94% of CaM still associates with MD-IQ1 in Ca^{2+} conditions relative to that under EGTA con-

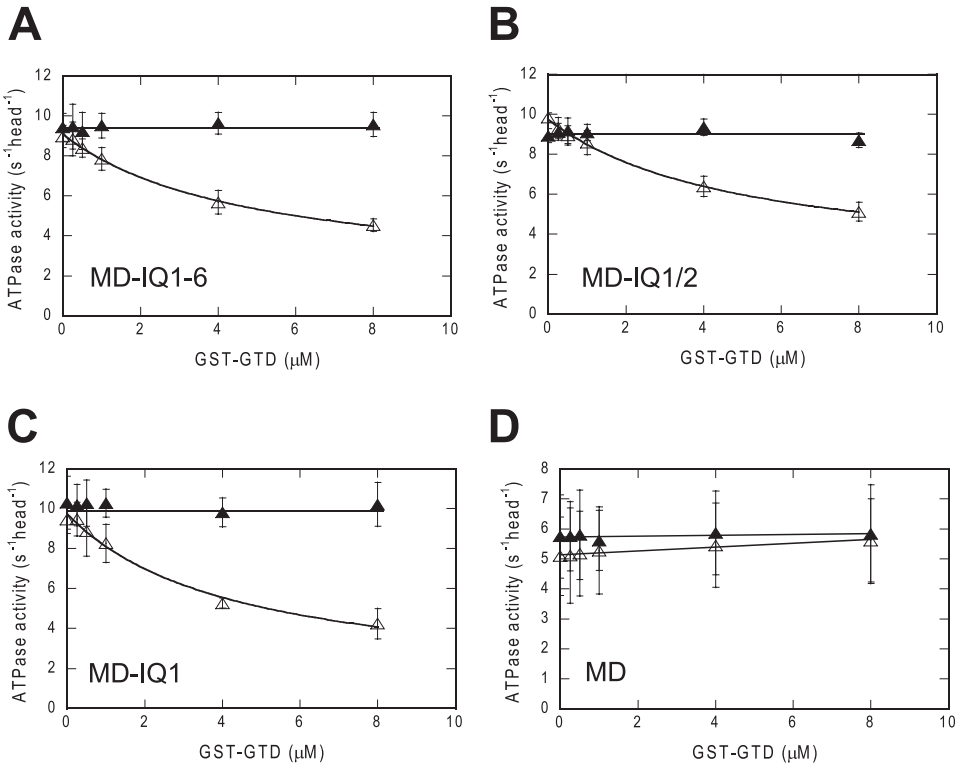

FIGURE 2. **Effects of IQ motif deletions on the inhibition of myosin 5a S1 ATPase activity by GST-GTD.** The actin-activated ATPase activities of the truncated myosin 5a S1 were measured in EGTA (*open triangles*) and pCa4 conditions (*closed triangles*). Data are the average of three independent assays. (*A*) MD-IQ1–6, (*B*) MD-IQ1/2, (*C*) MD-IQ1, and (*D*) MD. The K_d of GST-GTD to myosin 5a S1 constructs were obtained by a hyperbolic fit. The calculated K_d are 5.08 ± 1.51 μM (MD-IQ1–6), 4.33 ± 0.99 μM (MD-IQ1/2), and 3.46 ± 1.04 μM (MD-IQ1). Values are mean ± S.D. from three independent assays.

ditions (supplemental Fig. S3), indicating that the reversal of GST-GTD inhibition of MD-IQ1 ATPase activity by Ca^{2+} is due to a conformational change of the CaM bound to IQ1.

The Unique Sequence of IQ1 Is Critical for the Ca^{2+} Regulation of Myosin 5a—The six IQ motifs in the neck of myosin 5a can be grouped into three semiindependent pairs, *i.e.* IQ1/2, IQ3/4, and IQ5/6. The neighboring IQ motifs within each pair are separated by 23 aa, and by 25 aa between pairs. Sequence alignment shows that the structures of three pairs resemble each other. As described above, IQ1 plays a key role in Ca^{2+}-dependent regulation of myosin 5a. However, it is not known whether or not the unique sequence of IQ1 is essential for the regulation. To test this notion, we replaced the IQ1 of MD-IQ1 with IQ3 or IQ5, producing MD-IQ3 or MD-IQ5, respectively (Fig. 1 and supplemental Fig. S5). We found that the ATPase activity of neither MD-IQ3 nor MD-IQ5 is inhibited by GST-GTD despite Ca^{2+} concentrations (Fig. 3, *D* and *E*), indicating that the unique sequence of IQ1 is essential for Ca^{2+} regulation.

Since all three types of mammalian myosin 5, *i.e.* myosin 5a (6–8), 5b (26), and 5c[4] are regulated by their GTD in a Ca^{2+}-dependent manner, it is likely that, similar to that of myosin 5a, IQ1 of myosin 5b and 5c also plays a critical role in Ca^{2+} regulation. Therefore, we compared the IQ1 sequences of 12 mammalian myosin 5 and identified a consensus sequence of IQ1: KϕRxx$\omega\phi$xIQKxϕRGWLxBxBψx, where x is any amino acid, B is a basic residue, ϕ is a hydrophobic residue, ψ is an aromatic residue, and ω is a small hydrophilic residue (Fig. 3*A*). The conserved residues KϕR in the N terminus are absent in both IQ3 and IQ5, and WL in the middle are absent in IQ3 (Fig. 3*B*). It is likely that these residues, conserved in IQ1 but absent in IQ3 or IQ5, are essential for Ca^{2+} regulation. Indeed, the crystal structure of myosin 5a IQ1/2 in complex with CaM (27) shows that the absolutely conserved residues of IQ1: R767, W780, and L781, form intimate interactions with the surface residues in the C-lobe of CaM (Fig. 3*C*). These interactions likely render CaM in a proper conformation to interact with the GTD in a Ca^{2+}-dependent manner.

The Two Ca^{2+} Binding Sites in the C-lobe of CaM Are Critical for the Regulation of Myosin 5a Motor Function—CaM contains four EF-hand type Ca^{2+}-binding sites with different affinities for Ca^{2+}: two high affinity Ca^{2+}-binding sites in the C-lobe and two low affinity Ca^{2+}-binding sites in the N-lobe (17, 18). It is not known which Ca^{2+}-binding site(s) is responsible for Ca^{2+}-regulation of myosin 5a. Mutagenesis studies have shown that the conserved glutamic acid residue at the 12th position of each Ca^{2+}-binding loop is critical for Ca^{2+} binding (28). Substitution of this conserved glutamic acid with glutamine in each Ca^{2+}-binding site abolishes its Ca^{2+} binding ability. To identify the Ca^{2+}-binding sites in CaM responsible for Ca^{2+} regulation of myosin 5a, we examined the GST-GTD inhibition of the ATPase activity of MD-IQ1 coexpressed with CaM variants in the absence and presence of Ca^{2+}.

We coexpressed MD-IQ1 heavy chain with CaM variants in sf9 cells and purified MD-IQ1 by anti-FLAG affinity chromatography. Similar to wild-type CaM (CaM-WT), each CaM mutants was copurified with MD-IQ1 heavy chain (Fig. 4). It is

[4] X. Li, unpublished observations.

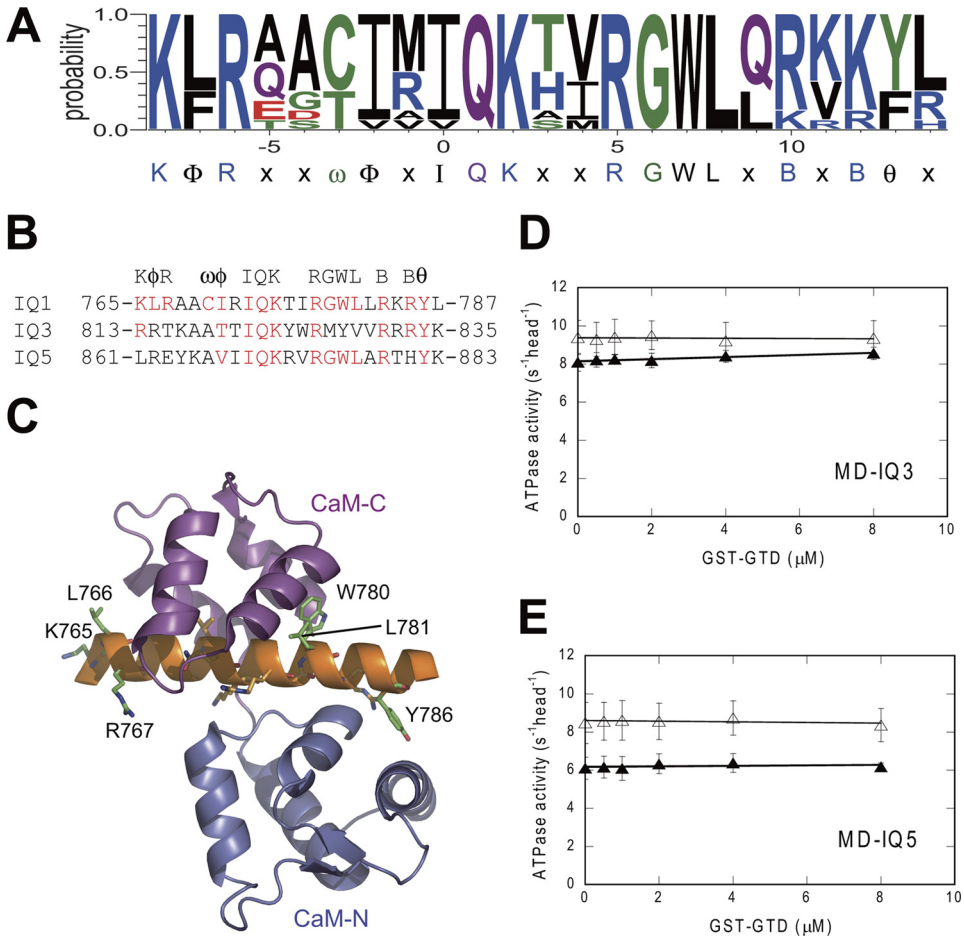

FIGURE 3. **Regulatory function of IQ1 cannot be substituted by IQ3 or IQ5.** *A*, consensus sequence of IQ1 motif of 12 mammalian myosin 5, including myosin 5a, 5b, 5c from mouse (GenBank™ ID: Q99104, NM_201600, XM_198225), rat (GenBank™ ID: Q9QYF3, P70569, EDL77808), cattle (GenBank™ ID XP_002691008, XP_002691008, XP_002691009), and human (GenBank™ ID: Q9Y4I1, Q9ULV0, Q9NQX4). X is any amino acid, B is a basic residue, ϕ is a hydrophobic residue, ψ is an aromatic residue, and ω is a small hydrophilic residue. *B*, sequence alignment of mouse myosin 5a IQ1, IQ3, and IQ5. *C*, ribbon drawing of apo-CaM (N-lobe, marine; C-lobe, *magenta*) in complex with IQ1 of muring myosin 5a (PDB # 2IX7). *Orange residues*, typical IQ motif residues IQ*XXX*RG*XXX*R; *green residues*, conserved IQ1residues identified in this report (K765, L766, R767, W780, L781, and Y786). *D* and *E*, effects of GST-GTD on the actin-activated ATPase activity of MD-IQ3 (*D*) and MD-IQ5 (*E*) in EGTA (*open triangles*) or pCa4 conditions (*closed triangles*). MD-IQ3 and MD-IQ5 were created by substitution of IQ1 in MD-IQ1 with IQ3 and IQ5, respectively. Values are the average of two independent assays.

known that CaM-WT and mutants display a characteristic electrophoretic mobility shift in response of Ca^{2+} (24). As shown in Fig. 4, CaM variants copurified with MD-IQ1 show the same pattern of mobility shift as the corresponding CaM variants. These results confirm that the CaM associated with the MD-IQ1 heavy chain in each preparation contains the expressed recombinant CaM mutant. It is noteworthy that the purified MD-IQ1/CaM-B34Q and MD-IQ1/CaM-B1234Q contain significant amounts of sf9 endogenous CaM (Fig. 4*B*), although the expression levels of CaM-B34Q and CaM-B1234Q in these preparations are similar to those of CaM-B12Q or CaM-WT. We found that increasing the expression of CaM-B34Q or CaM-B1234Q cannot eliminate the association of endogenous CaM with MD-IQ1, indicating that the affinity between CaM-B34Q or CaM-B1234Q and MD-IQ1 is significantly weaker than that between CaM-WT or CaM-B12Q and MD-IQ1. These results are consistent with the crystal structure of myosin 5a IQ1/2 complexed with CaM, which shows that the binding of CaM to IQ is largely via the interactions between the C-lobe of CaM and the IQ motif (29).

We examined the effects of GST-GTD on the ATPase activities of MD-IQ1 coexpressed with CaM mutants in EGTA and pCa4 conditions. Similar to that of MD-IQ1 with CaM-WT, the ATPase activity of MD-IQ1 with CaM-B12Q was strongly inhibited by GST-GTD in the absence of Ca^{2+} but not in the presence of Ca^{2+} (comparing Figs. 2*C* and 5*A*). By contrast, the ATPase activity of MD-IQ with CaM-B34Q or -B1234Q was slightly inhibited by GST-GTD in the absence or presence of Ca^{2+} conditions (Fig. 5, *B* and *C*). These results indicate that the Ca^{2+}-binding sites in the C-lobe of CaM are responsible for Ca^{2+}-dependent regulation of myosin 5a.

The presence of a population of wild type MD-IQ1/CaM in MD-IQ1/CaM-B34Q and MD-IQ1/CaM-B1234Q should not affect the ATPase assay results of these two constructs. First, the excess amount of CaM mutants in the assay could replace wild type CaM and restore the normal stoichiometry for MD-IQ1/CaM-B34Q and MD-IQ1/CaM-B1234Q. To test this possibility, we incubated MD-IQ1/CaM-B34Q or MD-IQ1/CaM-B1234Q with 12 μM corresponding CaM mutant and precipitated MD-IQ1 with F-actin. The CaM coprecipitated with

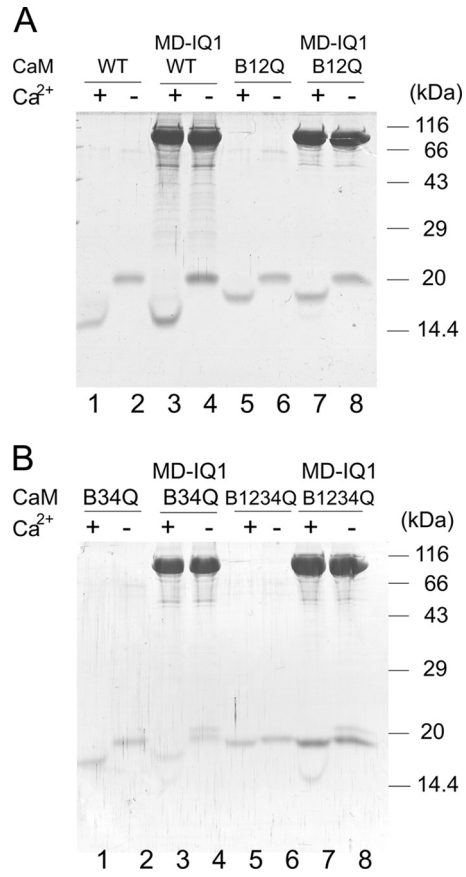

FIGURE 4. **Electrophoretic mobility shift of CaM mutants in the presence of EGTA or Ca^{2+} conditions.** *A*, *lanes 1* and *2*, wild type CaM; *lanes 3* and *4*, MD-IQ1 with wild type CaM; *lanes 5* and *6*, CaM-B12Q; *lanes 7* and *8*, MD-IQ1 with CaM-B12Q. *B*, *lanes 1* and *2*, CaM-B34Q; *lanes 3* and *4*, MD-IQ1 with CaM-B34Q; *lanes 5* and *6*, CaM-B1234Q; *lanes 7* and *8*, MD-IQ1 with CaM-B1234Q.

MD-IQ1 was analyzed by SDS-PAGE and the stoichiometry of light chain *versus* heavy chain was quantified (Fig. 5*D*). For MD-IQ1/CaM-B34Q, this treatment increased the stoichiometry of CaM-B34Q from 0.14 to 0.84, while it decreased that for wild type CaM from 0.19 to 0.07. For MD-IQ1/CaM-B1234Q, this treatment increased the stoichiometry of CaM-B1234Q from 0.59 to 0.90, while it decreased that for wild type CaM from 0.15 to 0.03. Second, if a population of wild-type MD-IQ1/CaM in the ATPase assay is significantly present, we should have seen a Ca^{2+}-dependent inhibition by GST-GTD similar to Fig. 2*C*.

It is known that the N-lobe and the C-lobe of CaM, forming distinct globular domains, bind Ca^{2+} and undergo Ca^{2+}-dependent conformational changes independently. Since the interactions between CaM and IQ1 are largely via the C-lobe of CaM and the N-terminal portion of IQ1 (Fig. 3*C*), it is possible that the C-lobe of CaM is sufficient for the Ca^{2+} regulation of myosin 5a. To test this possibility, we coexpressed MD-IQ1 with CaM-C (the C-lobe of CaM, aa 80–148) and purified MD-IQ1 with anti-FLAG affinity chromatography. However, we found that purified MD-IQ1 contains significant amounts of sf9 endogenous CaM but not CaM-C (*lane 1* in supplemental Fig. S6). These observations indicate that the affinity between CaM-C and IQ1 is much weaker than that between CaM-WT and IQ1. The lower affinity between CaM-C and IQ1 is likely due to the absence of a weak interaction between the N-lobe of CaM and the C-terminal portion of IQ1. Since the C-lobe of CaM binds to the N-terminal portion of IQ1 and the N-lobe of CaM binds to the C-terminal portion of IQ1, it is possible to weaken the affinity between CaM-WT and IQ1, while maintaining the affinity between CaM-C and IQ1, by truncating the C terminus of IQ1. Therefore, we prepared a number of truncated MD-IQ1 and found that one of them, *i.e.* MD-IQ1-short (aa 1–783), was copurified with neither sf9 endogenous CaM nor the coexpressed CaM-C (*lane 3* in supplemental Fig. S6).

We then measured the inhibition of the ATPase activity of MD-IQ1-short by GST-GTD in the presence of 12 μM CaM variants. In the presence of CaM-WT or CaM-C, GST-GTD inhibited the ATPase activity of MD-IQ1-short in a Ca^{2+}-dependent manner (Fig. 6, *B* and *D*). By contrast, GST-GTD had no inhibition activity either in the presence of CaM-N or in the absence of any CaM variants (Fig. 6, *A* and *C*). These results clearly demonstrated that the C-lobe of CaM is necessary and sufficient for mediating the regulation of myosin 5a by Ca^{2+}.

The ATPase levels of MD-IQ1-short in the absence of CaM and in the presence of CaM-N are significantly lower than that in the presence of CaM-WT or CaM-C (Fig. 6). One possible scenario is that the IQ1-short motif without the bound CaM interacts with the motor domain and inhibits its ATPase activity. The binding of CaM-WT or CaM-C to the IQ1-short motif prevents the interaction with the motor domain and restores the normal activity. The low activity of MD-IQ1-short in the presence of CaM-N is likely due to the low affinity of CaM-N to the IQ1-short motif.

There is an inherit Ca^{2+} dependence for the ATPase activity of MD-IQ1-short/CaM-N even when no GST-GTD is added (Fig. 6*C*). Since the ATPase acitivity of the motor domain *per se* is Ca^{2+}-independent, as shown for MD (Fig. 2*D*), the Ca^{2+} dependence of MD-IQ1-short/CaM-N is probably due to the different interactions between IQ1-short motif and CaM-N with or without Ca^{2+} bound, or due to the different affinities of IQ1-short motif to apo-CaM-N and to Ca^{2+}-CaM-N.

DISCUSSION

The Ca^{2+} Activation of Myosin 5a Is Initiated via the CaM in IQ1—The neck of myosin 5a contains six IQ motifs, the binding sites for CaM or CaM-like light chain. Since micromolar concentrations of Ca^{2+} stimulate the ATPase activity of myosin 5a and induce an open conformation (5–8), it is expected that activation is initiated by the binding of Ca^{2+} to CaM, which is bound to the IQ motifs of the myosin 5a heavy chain.

The six IQ motifs of myosin 5a can be grouped into three pairs, *i.e.* IQ1/2, IQ3/4, and IQ5/6. A number of crystal structures of myosin 5 IQ motif in complex with CaM or CaM-like light chain have been solved (27, 30–31). These structures permit building a model of the entire neck of myosin 5 (30), showing that there is little or no interaction between two light chains in the adjacent pairs. Thus CaM in IQ3/4 or IQ5/6 is unlikely to influence the conformation of CaM in IQ1/2, which would preclude their direct role in Ca^{2+}-dependent regulation. By contrast, there are non-polar interactions between CaM in IQ1 and in IQ2 (27). Thus it is possible that the Ca^{2+}-dependent regulation is initiated via the Ca^{2+} binding to the CaM in IQ1 or in

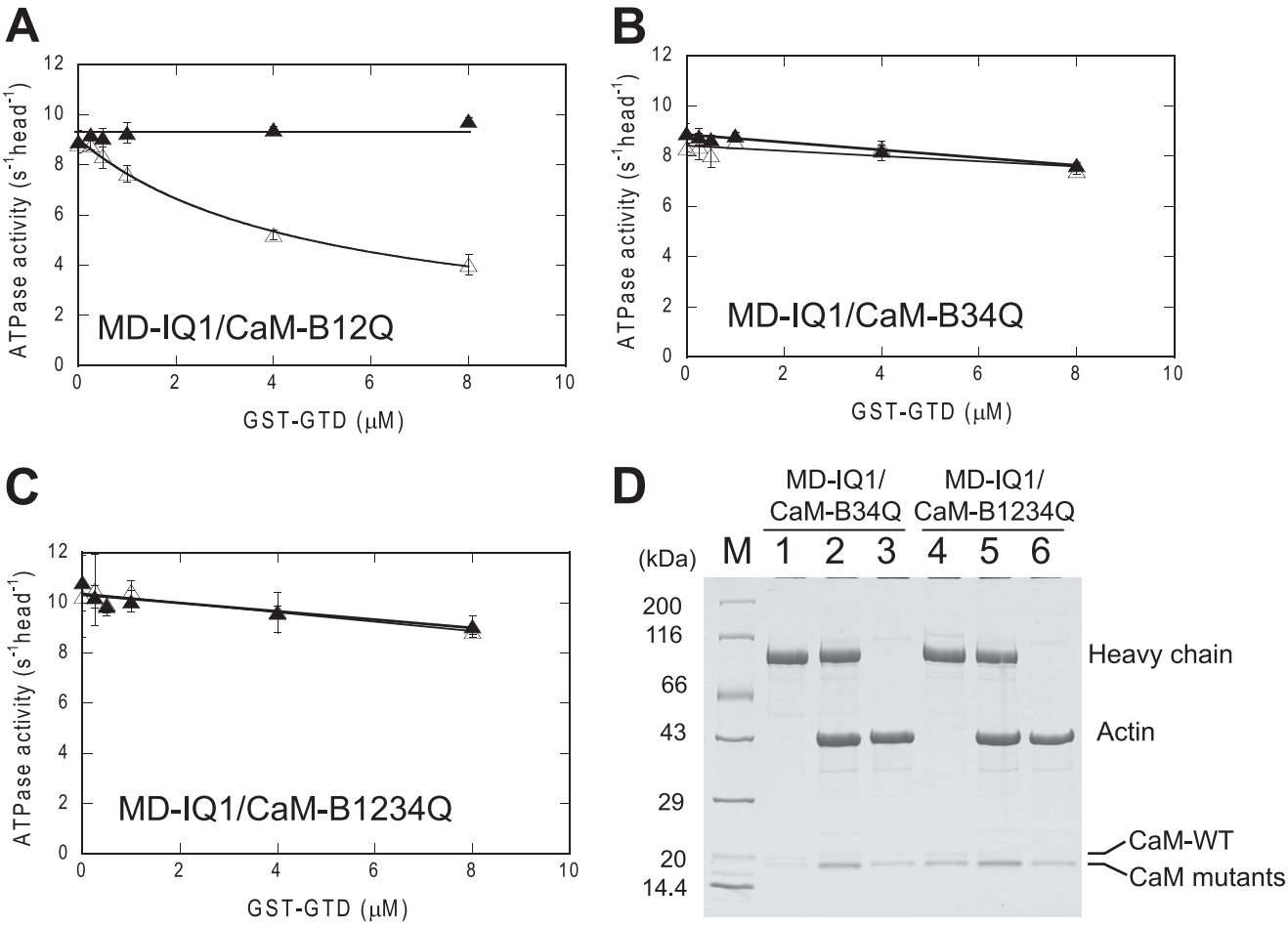

FIGURE 5. **The Ca^{2+}-binding sites in the C-lobe of CaM mediate the interaction between the head and the GTD.** The actin-activated ATPase activities of MD-IQ1 coexpressed with CaM mutants in the presence of various concentrations of the GST-GTD were measured. Assay conditions were conducted in the presence of 12 μM of the corresponding mutant CaM instead of wild-type CaM. *A*, MD-IQ1 with CaM-B12Q, (*B*) MD-IQ1 with CaM-B34Q, (*C*) MD-IQ1 with CaM-B1234Q. *Open triangles*, EGTA conditions; *closed triangles*, pCa4 conditions. Values are the average of two independent assays. *D*, exogenous CaM mutants restored the normal stoichiometry of light chain *versus* heavy chain for MD-IQ1/CaM-B34Q and MD-IQ1/CaM-B1234Q. Purified MD-IQ1/CaM-B34Q or MD-IQ1/CaM-B1234Q was incubated with 12 μM corresponding CaM mutant in EGTA conditions and subjected to actin cosedimentation and SDS-PAGE analysis. *Lanes 1* and *4*, MD-IQ1/CaM mutants prior to actin cosedimentation; *lanes 2* and *5*, MD-IQ1/CaM mutants after actin cosedimentation; *lanes 3* and *6*, CaM mutants control cosedimentated with actin. The stoichiometry of CaM WT or mutants coprecipitated with myosin 5a heavy chain was scored. For MD-IQ1/CaM-B34Q, the stoichiometry of CaM-WT and CaM-B34Q *versus* heavy chain are 0.14 and 0.19 prior to actin cosedimentation, and 0.07 and 0.84 after actin cosedimentation. For MD-IQ1/CaM-B1234Q, the stoichiometry of CaM-WT and CaM-B1234Q *versus* heavy chain are 0.15 and 0.59 prior to actin cosedimentation, and 0.03 and 0.90 after actin cosedimentation.

IQ2. Results presented here clearly demonstrate that the dissociation or conformational change of the CaM in IQ2 is not required for Ca^{2+} activation, and that the CaM in IQ1 is responsible for Ca^{2+}-dependent regulation of myosin 5a.

IQ2 in vertebrate smooth muscle and nonmuscle myosin II is the binding site for the regulatory light chain (RLC), which plays a key role for the regulation. The phosphorylation of the RLC of smooth muscle and nonmuscle myosin II stimulates the motor activity of their motor domains. It is generally believed that the phosphorylation of RLC alters the head-head interaction, relieving inhibition (17–18, 32). Therefore a double-headed structure is essential for the regulation of these myosins. By contrast, IQ1 of myosin 5a and bound CaM plays a key role in regulation via altering head-tail interaction. A double-headed structure, although it does enhance the head-tail interaction of myosin 5a and thus its regulation (10), is not essential for the regulation of myosin 5a. Recent studies show that, similar to myosin 5a, several unconventional myosins, including *Drosophila* myosin 7a and mammalian myosin 10, are auto inhibited by their tails and inhibitions are reversed by Ca^{2+} or cargo binding (33–36). Since these unconventional myosins cannot form stable double-headed structures as smooth muscle and nonmuscle myosin II, it is plausible that their first IQ motif occupied by CaM is responsible for Ca^{2+} regulation.

The Unique Interaction between CaM and IQ1 Is Essential for the Ca^{2+} Regulation of Myosin 5a—The overall conformations of myosin 5a IQ motif with bound CaM are very similar: the IQ motifs form a relatively straight α-helix with no sharp bend, and the C-lobe of CaM adopts a semi-open conformation that wraps around one side of IQ motif by forming strong interaction with the IQ motif, whereas the N-lobe adopts a closed conformation that interacts more weakly with the second part of the motif. However, the precise conformations of IQ-bound CaM are quite different. Comparing the structures of CaM/IQ1 and CaM/IQ2 reveals that variable residues of the IQ motif play a critical role in determining the precise conformation of the

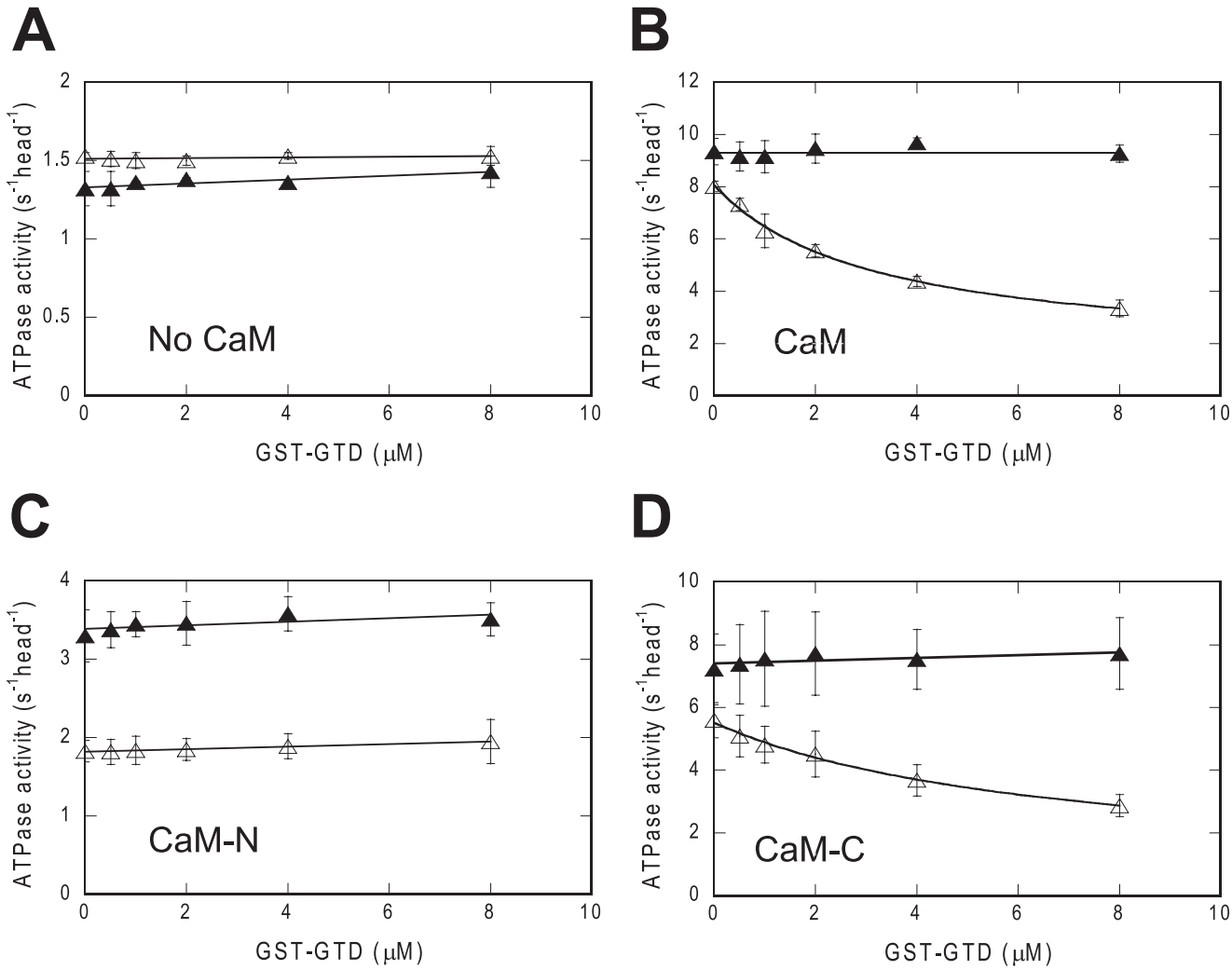

FIGURE 6. **The C-lobe of CaM is necessary for mediating the Ca^{2+}-dependent regulation of myosin 5a.** The actin-activated ATPase activities of MD-IQ1-short in the presence of various concentrations of the GST-GTD were measured in the absence of CaM variants (*A*), in the presence of 12 μM of CaM (*B*), CaM-N (*C*), or CaM-C (*D*). *Open triangles*, EGTA conditions; *closed triangles*, pCa4 conditions. Values are the average of two independent assays.

bound CaM and that conserved consensus residues of different IQ motifs can show unique interactions with CaM (27). Indeed, we identified a consensus sequence of IQ1 in addition to the typical IQ motif sequence of IQ*XXX*R*G**XXX*R. We propose that the N-terminal KϕR of IQ1 (where ϕ is a hydrophobic residue) and WL in the middle of IQ1 play the key roles in rendering CaM in a proper conformation to interact with GTD in a Ca^{2+}-dependent manner.

Although both apo- and Ca^{2+}-CaM bind tightly to IQ1 of Myosin 5a, it is likely that the binding interface between Ca^{2+}-CaM and IQ1 is quite different from that between apo-CaM and IQ1. The crystal structure of myosin 5a IQ1/2 bound to apo-CaM shows that the C-lobe of CaM adopts a semi-open conformation that grips the first part of the IQ motif, whereas the N-lobe adopts a closed conformation that interacts more weakly with the second part of the motif (29). The C-lobe of apo-CaM in IQ1 cannot bind with Ca^{2+} without conformational rearrangement, as several residues essential for Ca^{2+} binding are incorrectly oriented (27, 29). Upon Ca^{2+} binding, CaM rearranges its interaction with IQ1 and its overall conformation, which in turn might disrupt the interaction between the C-lobe of CaM and the GTD. Consistent with this notion, using electron cryo-microscopy together with computer-based docking of crystal structures into three-dimensional reconstructions of actin decorated with myosin 5a motor domain-IQ1/2 complex, Trybus *et al.* found that Ca^{2+} induces the tilting and sliding up of the CaM in IQ1 (16). However, the resolution of that structure is not high enough to show the detailed interaction between Ca^{2+}-CaM and IQ1. Resolving the structure of myosin 5 IQ1 bound with Ca^{2+}-CaM should reveal how Ca^{2+} induces the conformational transition of CaM in IQ1 and reverses the inhibition by the GTD.

The Interaction between the Head of Myosin 5a and the GTD—It is well established that in the inhibited state myosin 5a forms a compact triangular conformation in which the two globular tail domains directly interact with two head domains (7, 9–11). We previously identified a conserved acidic residue, D136, in the motor domain and two conserved basic residues, K1706 and K1779, in the GTD as the key residues for the interaction between the head and the GTD (11). Based on these findings, we propose that D136 in the motor domain and K1706/K1779 in the GTD form ionic interactions.

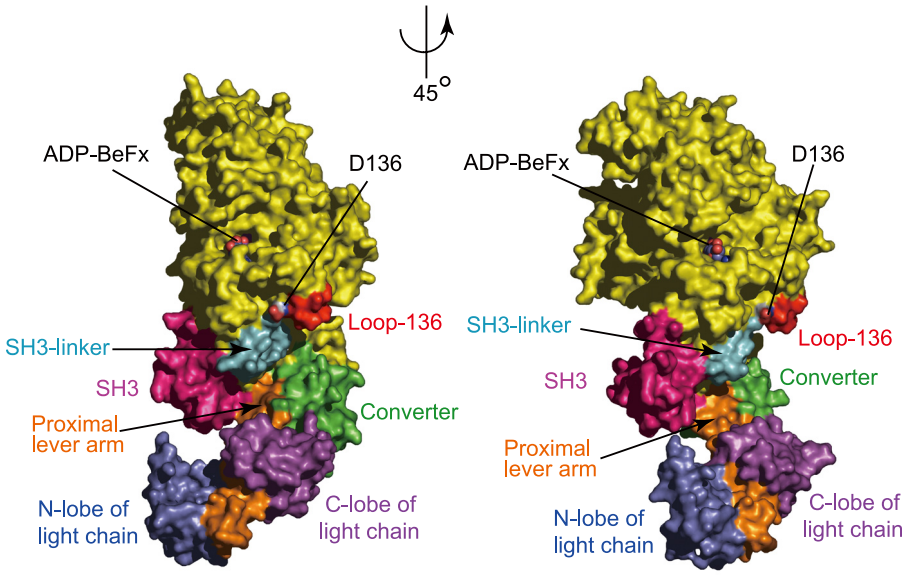

FIGURE 7. **The putative GTD binding site in the head of myosin 5a.** Surface of chicken myosin 5a motor domain and IQ1 in complex with LC1-sa, a CaM-like light chain (PDB # 1W7J) are colored *yellow* with following exception: *pink*, SH3 domain (A2-N64); *cyan*, the SH3-linker (P65-L77); *red*, loop-136 (G129-D136), *green*, the converter (S701-A753); *orange*, lever-arm (G754-R792); *marine*, the N-lobe of light chain, and *magenta*, the C-lobe of light chain. The putative GTD binding site is composed of the SH3-linker, loop-136, the converter, the proximal portion of lever-arm (G754-D765), and the C-lobe of CaM.

In the present study, we demonstrated that the C-lobe of CaM in IQ1 is essential for the inhibition of motor function by the GTD in a Ca^{2+}-dependent manner and we proposed that the C-lobe of CaM in IQ1 directly interact with the GTD in the absence of Ca^{2+}. In light of our new findings, we propose that the GTD binds to a shallow pocket in the head of myosin 5a formed by SH3-linker (P65-L77), loop-136 (G129-D136), converter (S701-A753), proximal portion of lever arm (G754-D765) (based on chicken myosin 5a sequence), and the C-lobe of CaM (Fig. 7). It is noteworthy that the model was done with chicken myosin 5a motor domain with IQ1 in complex with LC1-sa (a CaM-like light chain), the only available crystal structure of myosin 5a in complex with light chain. Although it was proposed that the light chain bound to IQ1 is LC1-sa but not CaM (37), a recent study showed that the light chain bound to IQ1 of chicken myosin 5a is actually CaM (15). We propose that the interaction between the head and the GTD includes, but not exclusively, the ionic interaction between D136 in the motor domain and K1706/1779 in the GTD and the interaction between the C-lobe of apo-CaM in IQ1 and the GTD. The putative GTD binding surface, except the converter, is highly conserved in vertebrate myosin 5. Thus it is likely that the converter determines the specificity of the interaction between myosin 5 head and its own GTD.

The Structure of the Inhibited Myosin 5a—The folded conformation of myosin 5a in the inhibited state can be visualized by negative staining electron microscopy and detected by analytical ultracentrifugation, indicating that the folded conformation is quite stable. It is likely that multiple intramolecular interactions between the head and the tail are involved. We previously demonstrated that the C-terminal end of the first coiled-coil segment (coil-1) of myosin 5a is essential for the folded conformation and proposed the interaction between this segment and the GTD (10). Consistently, we found here that the apparent affinity of GST-GTD for the HMM (having intact coil-1) is ~300-fold stronger than for the single-headed constructs, such as MD-IQ1–6 (having coil-1 deleted). Therefore at least two interactions contribute to the folded conformation of the inhibited myosin 5a: the interaction between the two heads and two GTDs and the interaction between the C-terminal end of coil-1 and the GTD. The interaction between the head and the GTD includes the ionic interaction between D136 in the motor domain and K1706/1779 in the GTD (11) and the interaction between the C-lobe of CaM in IQ1 and the GTD (this study). It should be noted that above two interactions are essential for the inhibition of myosin 5a as deletion of either interactions abolishes the inhibition by the GTD. On the other hand, the interaction between the GTD and the C-terminal end of coil-1 plays an auxiliary role for the inhibition, since deletion of this interaction only attenuates but not abolishes the inhibition by the GTD (10).

Based on above observation, we refine our model for the triangular conformation of the inhibited myosin 5a as following: GTD binds to the C-terminal end of coil-1; the neck-tail junction of myosin 5a is flexible and the long neck enables the head to reach the GTD associated at the end of coil-1; both the motor domain and the C-lobe of CaM in IQ1 interact with the GTD; once the heads interact with the GTD, the triangular inhibited conformation is stabilized. Of course, a conclusive picture of head-tail interaction will require the resolving of the crystal structure of the inhibited myosin 5a.

Acknowledgments—We thank Dr. Paul Odgren (University of Massachusetts Medical School) and Dr. Albert Wang (Boston Biomedical Research Institute) for reading the manuscript.

REFERENCES

1. Wu, X. S., Rao, K., Zhang, H., Wang, F., Sellers, J. R., Matesic, L. E., Copeland, N. G., Jenkins, N. A., and Hammer, J. A., 3rd. (2002) Identification of an organelle receptor for myosin-Va. *Nat. Cell Biol.* **4,** 271–278

2. Wu, X., Wang, F., Rao, K., Sellers, J. R., and Hammer, J. A., 3rd. (2002) Rab27a is an essential component of melanosome receptor for myosin Va. *Mol. Biol. Cell* **13,** 1735–1749
3. Fukuda, M., and Kuroda, T. S. (2004) Missense mutations in the globular tail of myosin-Va in dilute mice partially impair binding of Slac2-a/melanophilin. *J. Cell Sci.* **117,** 583–591
4. Li, X. D., Ikebe, R., and Ikebe, M. (2005) Activation of myosin Va function by melanophilin, a specific docking partner of myosin Va. *J. Biol. Chem.* **280,** 17815–17822
5. Cheney, R. E., O'Shea, M. K., Heuser, J. E., Coelho, M. V., Wolenski, J. S., Espreafico, E. M., Forscher, P., Larson, R. E., and Mooseker, M. S. (1993) Brain myosin-V is a two-headed unconventional myosin with motor activity. *Cell* **75,** 13–23
6. Li, X. D., Mabuchi, K., Ikebe, R., and Ikebe, M. (2004) Ca^{2+}-induced activation of ATPase activity of myosin Va is accompanied with a large conformational change. *Biochem. Biophys. Res. Commun.* **315,** 538–545
7. Wang, F., Thirumurugan, K., Stafford, W. F., Hammer, J. A., 3rd, Knight, P. J., and Sellers, J. R. (2004) Regulated conformation of myosin V. *J. Biol. Chem.* **279,** 2333–2336
8. Krementsov, D. N., Krementsova, E. B., and Trybus, K. M. (2004) Myosin V: regulation by calcium, calmodulin, and the tail domain. *J. Cell Biol.* **164,** 877–886
9. Thirumurugan, K., Sakamoto, T., Hammer, J. A., 3rd, Sellers, J. R., and Knight, P. J. (2006) The cargo-binding domain regulates structure and activity of myosin 5. *Nature* **442,** 212–215
10. Li, X. D., Jung, H. S., Mabuchi, K., Craig, R., and Ikebe, M. (2006) The globular tail domain of myosin Va functions as an inhibitor of the myosin Va motor. *J. Biol. Chem.* **281,** 21789–21798
11. Li, X. D., Jung, H. S., Wang, Q., Ikebe, R., Craig, R., and Ikebe, M. (2008) The globular tail domain puts on the brake to stop the ATPase cycle of myosin Va. *Proc. Natl. Acad. Sci. U.S.A.* **105,** 1140–1145
12. Nascimento, A. A., Cheney, R. E., Tauhata, S. B., Larson, R. E., and Mooseker, M. S. (1996) Enzymatic characterization and functional domain mapping of brain myosin-V. *J. Biol. Chem.* **271,** 17561–17569
13. Homma, K., Saito, J., Ikebe, R., and Ikebe, M. (2000) Ca(2+)-dependent regulation of the motor activity of myosin V. *J. Biol. Chem.* **275,** 34766–34771
14. Trybus, K. M., Krementsova, E., and Freyzon, Y. (1999) Kinetic characterization of a monomeric unconventional myosin V construct. *J. Biol. Chem.* **274,** 27448–27456
15. Koide, H., Kinoshita, T., Tanaka, Y., Tanaka, S., Nagura, N., Meyer zu Hörste, G., Miyagi, A., and Ando, T. (2006) Identification of the single specific IQ motif of myosin V from which calmodulin dissociates in the presence of Ca^{2+}. *Biochemistry* **45,** 11598–11604
16. Trybus, K. M., Gushchin, M. I., Lui, H., Hazelwood, L., Krementsova, E. B., Volkmann, N., and Hanein, D. (2007) Effect of calcium on calmodulin bound to the IQ motifs of myosin V. *J. Biol. Chem.* **282,** 23316–23325
17. Ikebe, M. (2008) Regulation of the function of mammalian myosin and its conformational change. *Biochem. Biophys. Res. Commun.* **369,** 157–164
18. Lowey, S., and Trybus, K. M. (2010) Common structural motifs for the regulation of divergent class II myosins. *J. Biol. Chem.* **285,** 16403–16407
19. Burgess, S. A., Yu, S., Walker, M. L., Hawkins, R. J., Chalovich, J. M., and Knight, P. J. (2007) Structures of smooth muscle myosin and heavy meromyosin in the folded, shutdown state. *J. Mol. Biol.* **372,** 1165–1178
20. Spudich, J. A., and Watt, S. (1971) The regulation of rabbit skeletal muscle contraction. I. Biochemical studies of the interaction of the tropomyosin-troponin complex with actin and the proteolytic fragments of myosin. *J. Biol. Chem.* **246,** 4866–4871
21. Seperack, P. K., Mercer, J. A., Strobel, M. C., Copeland, N. G., and Jenkins, N. A. (1995) Retroviral sequences located within an intron of the dilute gene alter dilute expression in a tissue-specific manner. *EMBO J.* **14,** 2326–2332
22. Ikura, M., Marion, D., Kay, L. E., Shih, H., Krinks, M., Klee, C. B., and Bax, A. (1990) Heteronuclear 3D NMR and isotopic labeling of calmodulin. Towards the complete assignment of the 1H NMR spectrum. *Biochem. Pharmacol.* **40,** 153–160
23. Ikebe, M., Reardon, S., Schwonek, J. P., Sanders, C. R., 2nd, and Ikebe, R. (1994) Structural requirement of the regulatory light chain of smooth muscle myosin as a substrate for myosin light chain kinase. *J. Biol. Chem.* **269,** 28165–28172
24. Zhu, T., Beckingham, K., and Ikebe, M. (1998) High affinity Ca^{2+} binding sites of calmodulin are critical for the regulation of myosin Ibeta motor function. *J. Biol. Chem.* **273,** 20481–20486
25. Martin, S. R., and Bayley, P. M. (2004) Calmodulin bridging of IQ motifs in myosin-V. *FEBS Lett.* **567,** 166–170
26. Wang, Z., Edwards, J. G., Riley, N., Provance, D. W., Jr., Karcher, R., Li, X. D., Davison, I. G., Ikebe, M., Mercer, J. A., Kauer, J. A., and Ehlers, M. D. (2008) Myosin Vb mobilizes recycling endosomes and AMPA receptors for postsynaptic plasticity. *Cell* **135,** 535–548
27. Houdusse, A., Gaucher, J. F., Krementsova, E., Mui, S., Trybus, K. M., and Cohen, C. (2006) Crystal structure of apo-calmodulin bound to the first two IQ motifs of myosin V reveals essential recognition features. *Proc. Natl. Acad. Sci. U.S.A.* **103,** 19326–19331
28. Beckingham, K. (1991) Use of site-directed mutations in the individual Ca2(+)-binding sites of calmodulin to examine Ca2(+)-induced conformational changes. *J. Biol. Chem.* **266,** 6027–6030
29. Coureux, P. D., Sweeney, H. L., and Houdusse, A. (2004) Three myosin V structures delineate essential features of chemo-mechanical transduction. *EMBO J.* **23,** 4527–4537
30. Terrak, M., Rebowski, G., Lu, R. C., Grabarek, Z., and Dominguez, R. (2005) Structure of the light chain-binding domain of myosin V. *Proc. Natl. Acad. Sci. U.S.A.* **102,** 12718–12723
31. Terrak, M., Wu, G., Stafford, W. F., Lu, R. C., and Dominguez, R. (2003) Two distinct myosin light chain structures are induced by specific variations within the bound IQ motifs-functional implications. *EMBO J.* **22,** 362–371
32. Wendt, T., Taylor, D., Trybus, K. M., and Taylor, K. (2001) Three-dimensional image reconstruction of dephosphorylated smooth muscle heavy meromyosin reveals asymmetry in the interaction between myosin heads and placement of subfragment 2. *Proc. Natl. Acad. Sci. U.S.A.* **98,** 4361–4366
33. Yang, Y., Baboolal, T. G., Siththanandan, V., Chen, M., Walker, M. L., Knight, P. J., Peckham, M., and Sellers, J. R. (2009) A FERM domain autoregulates *Drosophila* myosin 7a activity. *Proc. Natl. Acad. Sci. U.S.A.* **106,** 4189–4194
34. Umeki, N., Jung, H. S., Watanabe, S., Sakai, T., Li, X. D., Ikebe, R., Craig, R., and Ikebe, M. (2009) The tail binds to the head-neck domain, inhibiting ATPase activity of myosin VIIA. *Proc. Natl. Acad. Sci. U.S.A.* **106,** 8483–8488
35. Umeki, N., Jung, H. S., Sakai, T., Sato, O., Ikebe, R., and Ikebe, M. (2011) Phospholipid-dependent regulation of the motor activity of myosin X. *Nat. Struct. Mol. Biol.* **18,** 783–788
36. Sakai, T., Umeki, N., Ikebe, R., and Ikebe, M. (2011) Cargo binding activates myosin VIIA motor function in cells. *Proc. Natl. Acad. Sci. U.S.A.* **108,** 7028–7033
37. De La Cruz, E. M., Wells, A. L., Sweeney, H. L., and Ostap, E. M. (2000) Actin and light chain isoform dependence of myosin V kinetics. *Biochemistry* **39,** 14196–14202